14Cr-ODS Steel Produced by SPS from Mechanical Milled Powders with High Efficiency Oxide Precursors Incorporation

E. Macía (Universidad Carlos III de Madrid, Av. Universidad 30, 28911 Leganés, Madrid, Spain)

Abstract
Currently, one of the biggest issues when developing an ODS alloy is the competition established between the different oxide precursors during the precipitation of oxides which nature depends on their chemical composition. In the presence of various precursors, usually the one with the highest affinity to oxygen leads to the absence of the other oxides. In this work, a new process to equilibrate the local concentration of species and to decrease the competition among them is explained. A unique compound, containing the diverse oxide precursors as one complex oxide, is introduced in a prealloyed 14Cr Steel powder via mechanical alloying. Thus, generating environments enriched in Y, Ti and Zr which, after consolidation, refine the oxides precipitation improving the thermal stability of the alloy. SPS were used as consolidation technique to guarantee shorter sintering times and to maintain the nanostructure obtained. Mechanical properties were tested by tensile tests and Vickers microhardness.

Keywords: ODS steel, Mechanical Alloying, Spark Plasma Sintering, Zirconium, co-precipitation.

Introduction

Oxide Dispersion Strengthened (ODS) ferritic Steels are one of the options to be used in nuclear energy applications especially on those component expose to higher operation temperatures. Their good mechanical properties result from the high oxide dispersion into the ferritic matrix, whose pinning effect and high stability at high temperature improve the creep behaviour. Traditionally, those oxides were produced by the addition of one oxide precursor (Y_2O_3), and pure elements such as Ti, Zr, whose reaction during the milling step, and further precipitation during the consolidation allowed the formation of those nanoclusters and nano-oxides. The competition established by the different oxides precursors depends directly on the affinity of the different elements with the oxygen that results in the production of different oxides with an uncertain stoichiometry. In the Al containing ODS steels, Al is introduced to optimize the corrosion behaviour by the formation of Al_2O_3 layers. However, Y-Al-O oxides were produced during the consolidation step. Trying to modify the amount of this kind of oxides, some researchers have decided to introduce TiH_2 nanoparticles. The reactive behaviour of this compound can promote more coherent oxides and more stable at high temperatures, or directly form Y-Ti-O seeking for the same objective [1], [2] Other options are studying the use of Zr (or ZrO_2) to improve the thermal stability by refining the oxides precipitation [3]–[7].

The innovation aspect proposed in this research is to produce a complex nano-oxide Y-Ti-Zr-O by using a co-precipitation method. To synthetize the complex nanoparticles, liquid precursor routes are promising options to mix homogeneously the elements at a molecular scale. Once the precursor oxide is synthesized, to obtain an ODS steel those nano-oxides will be introduced in a 14Cr Ferritic steel, by using Mechanical alloying (MA) and subsequent consolidation by Spark Plasma Sintering (SPS). The aim is to facilitate and refine the precipitation of nano-oxides after the consolidation of MA powders, the idea is to generate by high energy milling local environments enriched on these elements Y-Ti-Zr [8]. The consolidation behaviour is also reported, looking for a competitive ODS steel using this new method of production.

Experimental procedure

Synthesis of nano oxides Y-Ti-Zr-O powders was carried out by co-precipitation using the precursors yttrium nitrate, titanium isopropoxide and zirconium n-butoxides. Each precursor was diluted individually in 5 ml of isopropanol to avoid unexpected segregations on the next step. After that, the three dissolutions were mixed in aqueous solution keeping at 10 pH by the addition of concentrated NH_4OH [8]. The co-precipitation continued for one hour. To eliminate all the residues produced during the co-precipitation, the resultant precipitates powders were filtered out, washed several times by using distilled water and a mixture of methanol and ethanol in equal proportion (50% in vol.). Then, the powders were dried in a hot plate, and pyrolised at 700°C for one hour in air. To crystallize the powders, another thermal treatment was performed at 850 °C during 30 min using a heating rate of 10 K/min in air too.

After that, to control the powder composition after pyrolysis cycle, the carbon content was measured by using LECO CS230. The formation of compounds and analysis of phases in crystallized powders were estimated by using X–ray diffraction (XRD). The diffraction patterns were collected by using X-ray Diffractometer (Bruker AXS,D8Advance) with a step size of 0.009 and a step time of 612 seconds per step. The morphology, particle size and composition of the powder was analysed by using TEM FEG S/TEM (Talos F200X, FEI, USA) operated 200 KV. Samples were ultrasonically dispersed in acetone suspensions, to deposit a drop on a coated carbon grid.

The ODS materials analysed in this research was obtained by using MA and SPS with the composition showed in table 1. A prealloyed powder Fe-14Cr-5Al-3W (Sandvik Osprey Powder Group) and the former nanoparticles produced by co-precipitation, Y-Ti-Zr-O, were the starting raw materials. The amount of complex oxide was calculated to keep the level of Y in 0,20 wt.% (analogous as 0.25wt% of Y_2O_3 addition).

Table 1. Chemical composition of the processed alloy.

	Prealloyed				Complex Oxide
	Fe	Cr	Al	W	Y-Ti-Zr-O
14YTiZrO	bal	14	5	3	0.96

The MA was performed in a horizontal ZOZ attritor Simloyer CM01 type under highly pure Argon atmosphere (99.9995 vol%) after a previous vacuum purge to control the quality of the atmosphere into the milling. The balls to powders ratio was 20:1, the rotation speed was set up to 800 rpm with an effective milling time of 50 h. For mixing previously the powders, an initial step of 2 h at 200 rpm was done. Milled powders were characterized by XRD to monitor the crystallite size and microstrain values with milling time (calculations based on Scherrer method). Experiments were conducted with a step size of 0.01° and step time of 612 seconds per steps. The interstitial composition (C, O and N) was determined by using LECO TCH 600 and LECO CS230. In order to know the particle size a particle size analyser (LA950, Horiba,Japan) with a laser beam was used. The MA powder morphology was also studied by FEG-SEM (FEI Teneo).

SPS was performed as described (Table 2) (FCT Systeme GmbH). The ODS powders were introduced into a 20 mm cylindrical graphite die and heated in vacuum (10^{-2}-10^{-3} mbar). The temperature was controled with a pyrometer system in the upper graphite punch. To avoid the graphite contamination, a high-purity (>99.97%) tungsten foil (25 lm thick) was used as a diffusion barrier during the sintering process [6].

The density of the material was study by using particle analysis method. The final microstructure was evaluated by SEM (FEI Teneo)..

Finally, the mechanical properties of the material were evaluated by using microhardness test using a total load of 200 g (Zwick Rockel microhardness, Indentec Hardness Testing Machines Limited, United Kingdom). The tensile tests were conducted by using miniature dog bone shape specimen [9]. To calculate the strain, the crosshead displacement was used. Tensile load was applied with a rate of 2 μm s^{-1}.

Table 2. Different cycles designed for consolidation.

Pressure (MPa)	**Holding time (min)**	**Heating rate (K/min)**	**Temperature (ºC)**
57	3 min	100	1100
			1150
			1200
		300	1180
			1150
			1200
		500	1150

Results and discussion

Characterization of the nano-oxide synthesized

Fig. 1 shows the TEM images and EDS mapping of precipitated powders. Mapping analysis gives evidence for a homogeneous distribution of the oxide formers (Y-Ti-Zr), hence a complex oxide was successfully produced. Besides, the synthetized nano-oxides have small particles sizes in the range of several nanometers (app. 20nm).

.

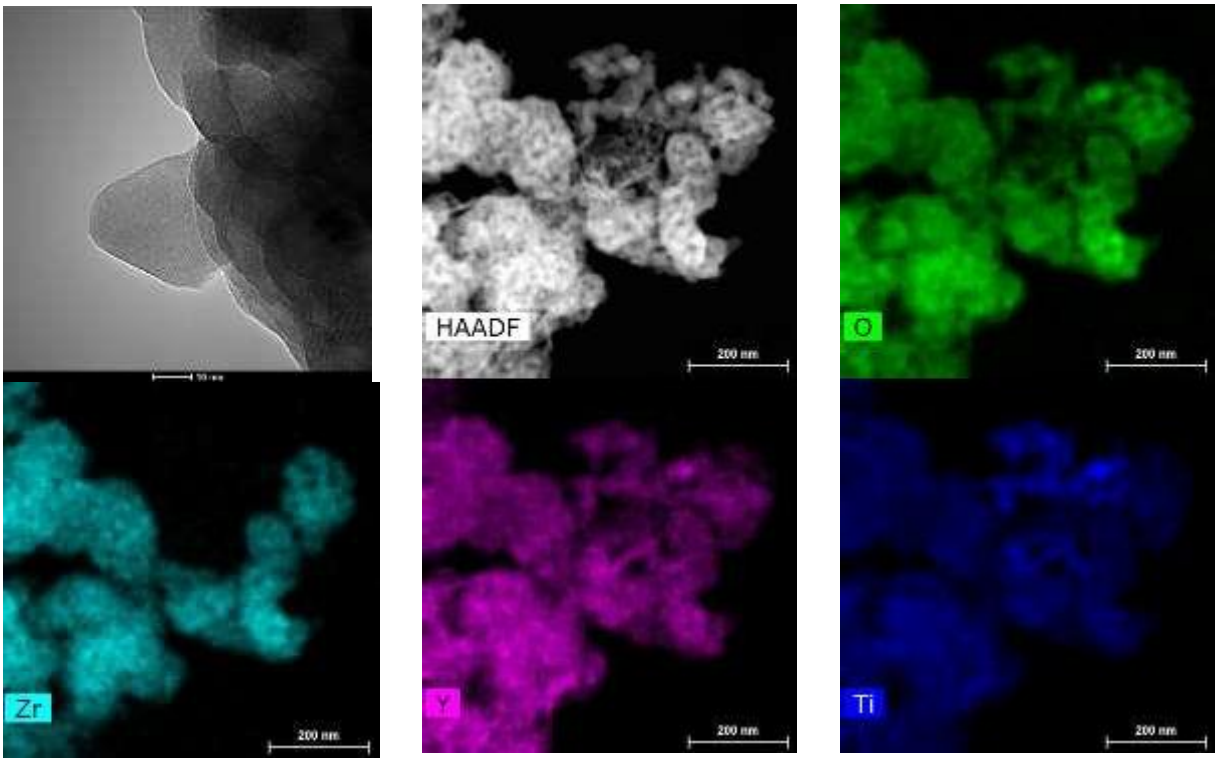

Fig. 1. Y-Ti-Zr-O STEM images of the nanopowder, high-angle annular dark-field imaging (HAADF) and EDS mapping analysis

X- ray characterization showed that the powder mainly fulfil a fluorite structure (Fig. 2) as it can be observed in the literature [8]. In addition, it is possible to detect some minority phases such as bixbyite and pyrochlore, ordered version of fluorite. All phases are favourable to produce a ODS steel since normally those are the kind of oxides present in the material by using traditional methods. During the co-precipitation there is a competition between Zr^{4+} and Ti^{4+} to obtain a final solid solution with fluorite structure, characterized by EDS as $Y_{0,9}Ti_{0,7}Zr_{2,2}O_{7,1}$. The C quantity has to be controlled during the co-precipitation to reduce the amount of interstitial in the final ODS steel. After pyrolysis the nanopowder has a 0,147 wt.% of C. This method opens a new way to control the presence of elements that can promote nano-oxides precipitation. Controlling the precipitation of minority phases and stoichiometry will be studied later on.

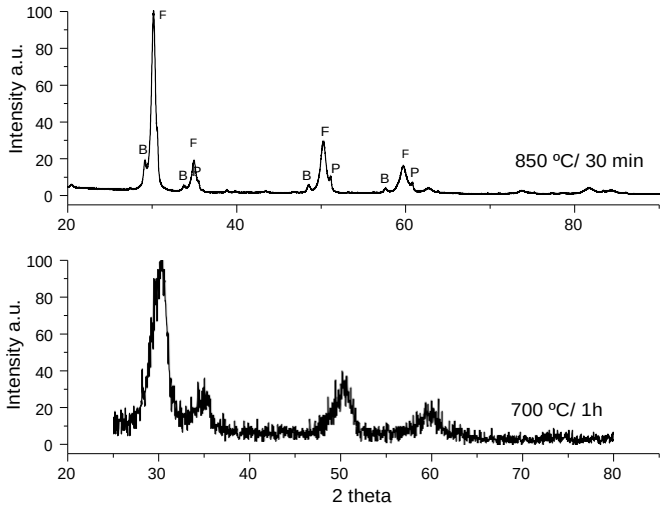

Fig 2. XRD of Y-Ti-Zr-O synthesised. Bixbyite and Pyrochlore are ordered version of Fluorite (target phase of the precipitated complex oxide) [8]

Characterization of the mechanical alloyed powder:
Prealloyed ferritic powder and nano-oxides were mechanically alloyed. The heavy deformation of the powders during mechanical alloying (fracture and re-welding) leads to structural changes of the iron matrix. The high dislocation density generated by MA decreases the coherence zone and as a result, the crystallite size of the material. At the same time, microstrain increases. The final values achieved are a crystallite size of 12 nm and a strain of 0.7 % respectively (Fig 3, left). Afterwards, the SEM study of MA powders shows an irregular morphology and sizes around 90-95 µm (Fig 3, right).

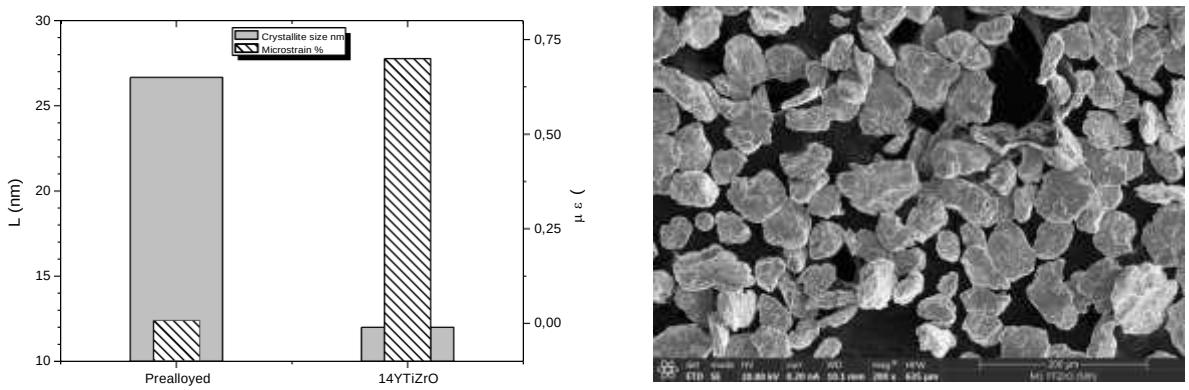

Fig 3. Left: structural parameters of prealloyed vs. MA powders, right: MA powder after introducing Y-Ti-Zr-O nano-oxides.

Characterization of the consolidated material
The different parameters used in SPS determine the final microstructure and the achieved density.. This work aims to discuss the effect of the final temperature and heating rate on the consolidated material.
First, selecting the heating rate at 100 K/min, temperatures were changed from 1100 ºC to 1200 ºC (Table 2). Keeping pressure and holding time constant, temperature influences the final densification of the material when the thermal activation is insufficient, in this case ≤1100 ºC (Fig 4, left).[10]. The relative density can be increased from 92% to 96% if the temperature was increased from 1110°C to 1200°C.

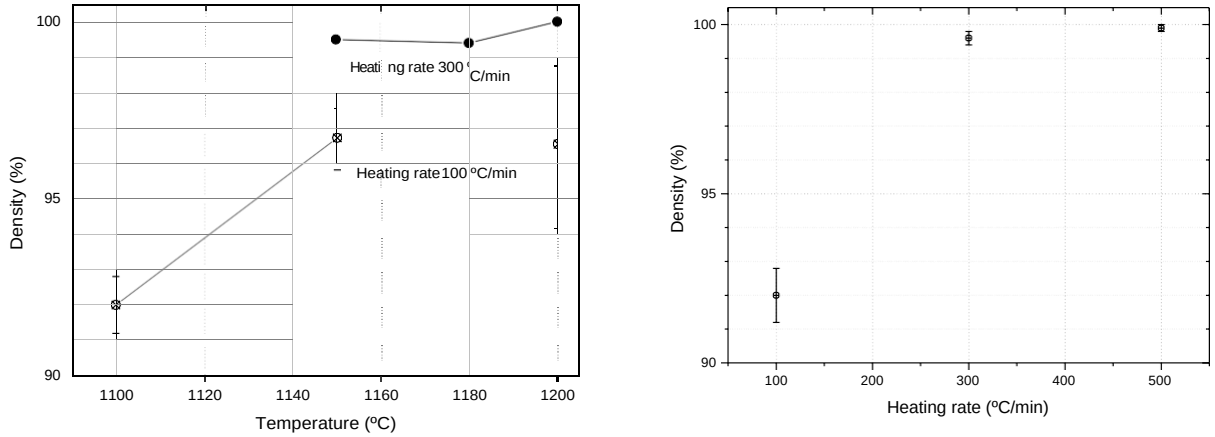

Fig 4. (Left) Density vs temperature and heating rate. Right: Density vs heating rate when SPS is performed up to 1150 ºC.

The heating rate seems to be the key parameter to obtain a fully dense material. If the heating rate was increased from 100 to 300 K/min, the specimens almost achieved full densification when temperature is set from 1150ºC to 1200ºC. However, at 1200 ºC and 300 K/min the reduction of the amount of ultrafine grains diminish the final mechanical properties, even if a total consolidation is achieved (see Fig 5, $HV_{0.2}$).

The objective is to suppress particle coarsening and enhance particle sintering. For this reason, to study the effect on the final densification the consolidation temperature was reduced at 1150 ºC and the heating

rate increased from 100 to 500 K/min (Fig. 4 right). As it can be observed in Fig 4, the density changes from 92 % to 99.8 %, these results prove the key effect of accelerating the heating. For increasing the heating rate, it was necessary to increase the current,.
The amount of heat released (Joule effect) is determined by the current flow, for this reason, if the current is increased the same is happening to the energy released. On the other side, an overall overheating (up to 100 K) could be promoted which can accelerate the powders diffusion and sintering. Achieving these conditions, it allowed to reduce the porosity between particles and finally to better consolidate the material (Fig. 5) [11][12]. The best sample was the one consolidated at 500 K/min.

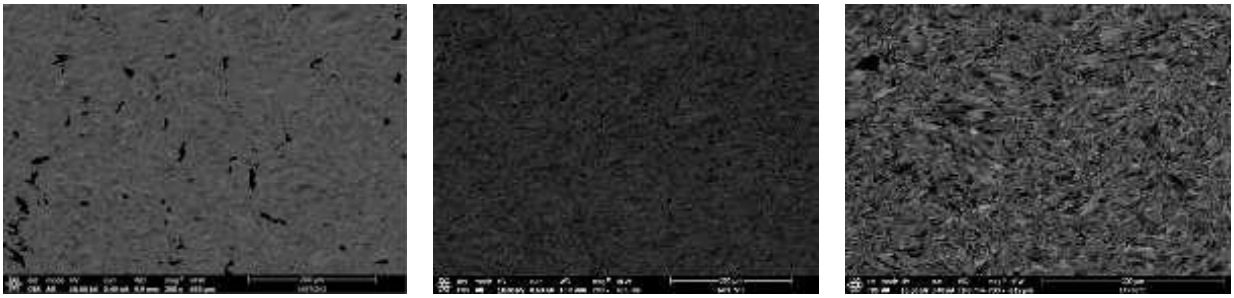

Fig. 5: Density evolution by changing the heating rate from 100, 300 and 500ºC/min (from left to right) when the maximum T is 1150ºC

A bimodal microstructure is obtained for all the conditions used. Fig 6 shows how large micrometrics grains surround the ultrafine grains. The abnormal growth is affected by the inhomogeneous and high deformation level achieved during the milling step, by the distribution and pinning effect of the nano-oxides dispersed into the matrix and by the accelerated consolidation method [13], [14]. The process in which the oxide formers are introduced (triple nano-oxide) is affecting the later precipitation (size, place and composition) and the way in which the oxides retain the grain and the stability of the final microstructure.

Besides, using different conditions in the SPS parameters have also an effect on the grain growth, especially on the ultrafine grains. Fig. 6 shows the two samples with the highest density, but the ultrafine colony size depends on the thermal activation. Considering the specimens processed up to 1200 °C - 300 K/min it can be noticed a decreased amount of ultrafine grain colonies and, consequently, the microhardness is reduced. Even so, the values obtained for both materials are comparable to the one reported in previous research [15].

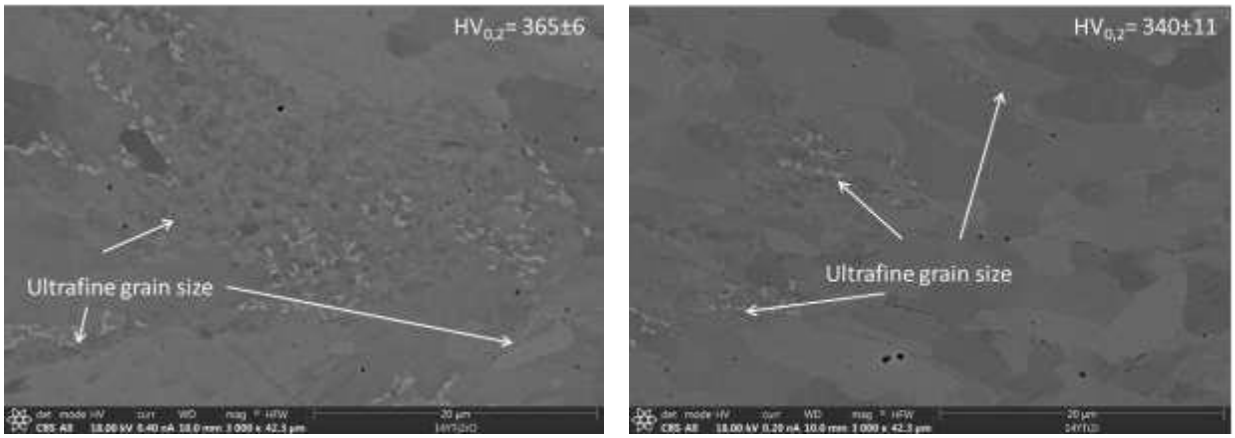

Fig. 6: Ultrafine grains :Left side (1150ºC,500ºC/min), right side (1200ºC,300ºC/min)

Microtensile test:
Microtensile tests were performed at the alloys consolidated at 1150°C, 500 K/min and 1200ºC, 300 K/min. The equilibrium achieved between the toughness (area under the curve) and ultimate tensile strength is interesting for future application under high temperatures.

The nano-oxides introduced retain the grain growth (leading to ultrafine-grained regions) and block the movements of dislocations, which result in this high UTS value. On the other side, the toughness is promoted by the high density and the micrograins present on the material. The amount of ultrafine grain colonies is reduced when SPS is performed up to 1200 ºC and 300 K/min, which explains the reduction in the UTS. On the other side, the toughness is almost the same, which speak about the effect of density and micrograins. Obtained tensile test values are similar to those obtained traditionally by introducing Y_2O_3, Ti, Zr [16]

Table 4. Tensile test properties at RT

Samples	UTS(MPa)	YS(MPa)	Toughness (MPa)	HR	Strain (%)
1200 °C,300 °C/min	935 ± 14	735 ± 25	190 ± 11	1,3	24,23 ± 1,79
1150 °C,500 °C/min	1001 ± 21	815 ± 18	177 ± 12	1,2	21,51 ± 1,38

Conclusions:

In this work an ODS steel has been obtained by MA with the addition of a complex oxide Y-Ti-Zr-O obtained by co-precipitation. It has been successful consolidated by using SPS as a consolidation technique. It was demonstrated that:

- Co-precipitation could be an effective method to obtain nanopowders with a determined composition. It allows to produce, rich environments in Y, Ti and Zr by high energy milling with a pre-alloyed ferritic stainless steel that should conditioned the later precipitation. Their pinning effect was studied in this research.
- SPS conditions can be optimized to obtain a fully dense material. The heating rate is the key factor that enables a full densification of the material.
- A bimodal grain was obtained for all the samples consolidated. The oxides produced, are effective on retaining the grain growth. Ultrafine colonies sizes depend on maximum T on SPS.
- The mechanical properties evaluated show the good behaviour of the ODS steel produce by this new method. The equilibrium achieved between UTS and toughness result to be interesting for its application under high temperatures.

Acknowledgments:

Authors want to acknowledge Ferro-Ness project and Ferro-Genesys project funded by MINECO under National I+D+I program MAT2016-80875-C3-3-R and MAT2013-47460-C5-5-P.

Bibliography:

[1] T. Liu, L. Wang, C. Wang, H. Shen, and H. Zhang, “Feasibility of using Y2Ti2O7 nanoparticles to fabricate high strength oxide dispersion strengthened Fe-Cr-Al steels,” *Mater. Des.*, vol. 88, pp. 862–870, 2015.

[2] L. Wang, Z. Bai, H. Shen, C. Wang, and T. Liu, “Creation of Y2Ti2O7 nanoprecipitates to strengthen the Fe-14Cr-3Al-2W steels by adding Ti hydride and Y2O3 nanoparticles,” *J. Nucl. Mater.*, vol. 488, pp. 319–327, 2017.

[3] Haijian Xu, Z. Lua, D. Wanga, and C. Liu, “Effect of zirconium addition on the microstructure and mechanical properties of 15Cr-ODS ferritic Steels consolidated by hot isostatic pressing,” *Fusion Eng. Des.*, vol. 114, pp. 33–39, Jan. 2017.

[4] H. Dong, L. Yu, Y. Liu, C. Liu, H. Li, and J. Wu, “Enhancement of tensile properties due to microstructure optimization in ODS steels by zirconium addition,” *Fusion Eng. Des.*, Apr. 2017.

[5] W. Li, T. Hao, R. Gao, X. Wang, T. Zhang, Q. Fang, and C. Liu, “The effect of Zr, Ti addition on the particle size and microstructure evolution of yttria nanoparticle in ODS steel,” *Powder Technol.*, vol. 319, pp. 172–182, Sep. 2017.

[6] A. García-Junceda, N. García-Rodríguez, M. Campos, M. Cartón-Cordero, and J. M. Torralba, “Effect of Zirconium on the Microstructure and Mechanical Properties of an Al-Alloyed ODS Steel Consolidated by FAHP,” *J. Am. Ceram. Soc.*, vol. 98, no. 11, pp. 3582–3587, 2015.

[7] L. Zhang, L. Yu, Y. Liu, C. Liu, H. Li, and J. Wu, “Influence of Zr addition on the microstructures and mechanical properties of 14Cr ODS steels,” *Mater. Sci. Eng. A*, vol. 695, pp. 66–73, May 2017.

[8] T. A. Schaedler, W. Francillon, A. S. Gandhi, C. P. Grey, S. Sampath, and C. G. Levi, “Phase evolution in the YO1.5-TiO2-ZrO2 system around the pyrochlore region,” *Acta Mater.*, vol. 53, no. 10, pp. 2957–2968, 2005.

[9] Y. H. Zhao, Y. Z. Guo, Q. Wei, T. D. Topping, A. M. Dangelewicz, Y. T. Zhu, T. G. Langdon, and E. J. Lavernia, “Influence of specimen dimensions and strain measurement methods on tensile stress-strain curves,” *Mater. Sci. Eng. A*, vol. 525, no. 1–2, pp. 68–77, 2009.

[10] Gibson, I., D. Rosen, and B. Stucker, Additive manufacturing technologies: 3D Printing. Rapid Prototyping, and Direct Digital Manufacturing, 2015.

[11] M. S. Staltsov, I. I. Chernov, I. A. Bogachev, B. A. Kalin, E. A. Olevsky, L. J. Lebedeva, and A. A. Nikitina, “Optimization of mechanical alloying and spark-plasma sintering regimes to obtain ferrite–martensitic ODS steel,” *Nucl. Mater. Energy*, 2016.

[12] A. S. Semenov, J. Trapp, M. Nöthe, O. Eberhardt, T. Wallmersperger, and B. Kieback, “Experimental and numerical analysis of the initial stage of field-assisted sintering of metals,” *J. Mater. Sci.*, vol. 52, no. 3, pp. 1486–1500, 2017.

[13] I. Hilger, X. Boulnat, J. Hoffmann, C. Testani, F. Bergner, Y. De Carlan, F. Ferraro, and A. Ulbricht, “Fabrication and characterization of oxide dispersion strengthened (ODS) 14Cr steels consolidated by means of hot isostatic pressing, hot extrusion and spark plasma sintering,” *J. Nucl. Mater.*, vol. 472, pp. 206–214, 2015.

[14] X. Boulnat, M. Perez, D. Fabregue, T. Douillard, M. H. Mathon, and Y. De Carlan, “Microstructure evolution in nano-reinforced ferritic steel processed by mechanical alloying and spark plasma sintering,” *Metall. Mater. Trans. A Phys. Metall. Mater. Sci.*, vol. 45, no. 3, pp. 1485–1497, 2014.

[15] Gibson, I., et al., Materials for Additive Manufacturing, in Additive Manufacturing Technologies. 2021, Springer, Cham. p. 379-428.

[16] N. García-Rodríguez, M. Campos, J. M. Torralba, M. H. Berger, and Y. Bienvenu, “Capability of mechanical alloying and SPS technique to develop nanostructured high Cr, Al alloyed ODS steels,” *Mater. Sci. Technol.*, vol. 30, no. 13b, pp. 1676–1684, 2014.

[17] E. Macia, J. Cornide, L. A. Diaz, and M. Campos, “Estudio de la evolución microestructural de una acero ferrítico ODS de grupo 4 (Y-Ti-Al-Zr) consolidado por consolidación Spark Plasma Sintering (SPS),” *VI Congr. Nac. pulvimetalurgia*, vol. 4, no. 978-84-697-3650–0, pp. 1–6, 2017.